A Broadband CPW-Fed Circularly Polarized Square Slot Antenna for UHF RFID Applications

Shaoshuai Zhang*, **He Huang, and Yingzeng Yin**

Abstract—A broadband CPW-fed circularly polarized square slot antenna for ultra-high-frequency (UHF) radio frequency identification (RFID) applications is proposed. It consists of a square slot embedded with a spur line along diagonal and an F-shaped feeding structure. The proposed antenna achieves an impedance bandwidth about 307 MHz (34.6% @886 MHz) and a 3 dB axial ratio (AR) bandwidth about 232 MHz (24.3% @954 MHz). The 3 dB AR beam-width is about 96 degrees over the UHF band of 840–960 MHz. The proposed reader antenna based on CPW structure is easy to integrate. With the symmetry and bidirectional radiation pattern, there are less readers needed in some applications, such as access control, than the reader with unidirectional pattern, which will definitely decrease the implemented cost. Therefore, this universal design with desired performance across the entire UHF RFID band (from 840 MHz to 960 MHz) can be applied to all the UHF RFID applications worldwide. Detailed considerations of the design and main parameters will be studied in this paper.

1. INTRODUCTION

Radio frequency identification (RFID) is a technique used for identification and tracking of objects by means of electromagnetic waves [1]. In recent years, RFID technology has been rapidly developed and applied to many service industries, distribution logistics, manufacturing companies, and goods flow systems [2–5]. The RFID system consists of an interrogator, namely the reader [6], and the tags [5] that contain relevant information of the objects they are attached. Compared to conventional identification method or barcodes, RFID technology offers several advantages, such as the ability of simultaneously reading a number of tags, higher reading range, and faster data transfer [7]. Generally speaking, the tag antennas are linearly polarized. Due to the random orientation of the tags in actual applications, a circularly polarized (CP) antenna for the RFID reader is required to get the most efficient UHF RFID system [8]. Globally, each country has its own frequency allocation for UHF RFID applications, e.g., 840.5–844.5 and 920.5–924.5 MHz in China, 866–869 MHz in Europe, 902–928 MHz band in North and South of America, 866–869 and 920–925 MHz in Singapore, 952–955 MHz in Japan, etc., so that the UHF RFID frequency ranges from 840.5 to 955 MHz (a fractional bandwidth of 12.75%) [8]. Circularly polarized RFID reader antennas with single port have been extensively studied [9–12]. Numerous CP reader antennas such as antenna comprising corner truncated patch and suspended micro-strip line [13], asymmetric-circular shaped slotted micro-strip antenna [14] and spirally complementary split-ring resonators antenna [15] have been presented. Whereas, the reader antennas mentioned above have the disadvantages of complex structure [16], narrow bandwidth [17], bulky volume [18] and unidirectional radiation pattern. The reader antenna with unidirectional radiation means that there are more readers needed in some applications, such as access control, than the reader with symmetrical bidirectional pattern, which definitely increases the implemented cost [19].

Therefore, a universal compact reader antenna with desired performance such as symmetrical bidirectional radiation pattern and wider 3 dB AR beam with moderate gain across the entire UHF

RFID band would be beneficial for RFID system configuration and implementation, as well as cost reduction. In this paper, a reader antenna consisting of the square slot embedded with a spur line along the diagonal fed by an F-shaped structure, which has advantages of simple structure and ease of integration because of its basis on the coplanar waveguide, is proposed. Due to the spur line which disturbs the surface electric field distribution on the square slot, two near-degenerated resonant modes with 90-degree phase difference are closely excited to form a wide CP operating bandwidth for UHF band. The obtained impedance bandwidth across the operating band can reach about 304 MHz (34.6% @886 MHz) and 3 dB AR bandwidth about 232 MHz (24.3% @954 MHz). Parametric study for the salient parameters of the proposed CP antenna is also conducted to give a further insight into the proposed antenna. All the structures were simulated and optimized by Ansoft high frequency structure simulator (HFSS v13.02).

2. PROPOSED ANTENNA CONFIGURATION

The geometry configuration and photograph of the proposed planar antenna is shown in Figure 1. The antenna was fabricated on a low-cost FR4 glass epoxy substrate with a thickness of 0.8 mm, a relative permittivity of 4.4 and a loss tangent of 0.02 and fed by CPW with its feeding point located at the edge of the antenna. The optimum dimensions are shown in Table 1. As indicated in Figure 1, the proposed antenna consists of an F-shaped feeding structure to obtain a wideband impedance bandwidth about 304 MHz (33.2% @887 MHz) and a square slot embedded with a spur line along the diagonal to excite two orthogonal degenerate resonant modes with 90-degree phase difference.

The square slot is set to 84 mm × 75 mm to degenerate TE_{10} and TE_{01} components of CP operation by etching a spur line to the square slot. Due to the spur line, which splits the dominant resonant mode
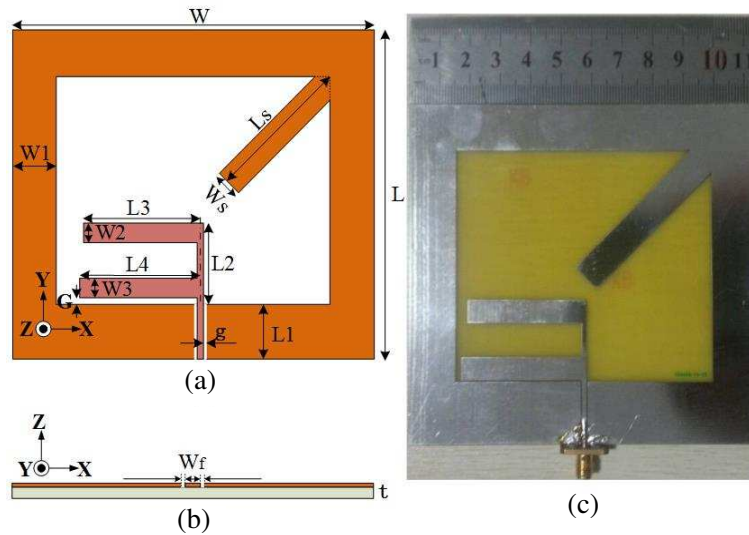
Figure 1. Geometry and photograph of the proposed planar broadband circularly polarized antenna. (a) Geometry (top view). (b) Geometry (side view). (c) Photograph.

Table 1. Optimum parameters of the proposed antenna (unit: mm).

W	L	W_1	W_2	W_3
114	110	15	7.5	7.5
W_s	L_s	L_1	L_2	L_3
10	58.5	20	26.5	38
L_4	G	g	t	W_f
40	0.5	0.4	0.8	1.48

into two orthogonal near-degenerated modes, the excited $\hat{x}$-directed electric field is lagged behind while the one in the $\hat{y}$-directed is slightly affected. Given a proper spur line length, these two orthogonal modes can achieve 90-degree phase difference, resulting in an LHCP radiation in $+\hat{z}$ direction while an RHCP in $-\hat{z}$ direction.

The operating frequencies 890 MHz and 1 GHz obtained by (1) were roughly the same as the frequencies 890 MHz and 1020 MHz where the lowest axial ratio was located as shown in Figure 3(b). With these two adjacent frequencies merged together, the AR bandwidth was enhanced.

$$f_c = \frac{c}{2\pi\sqrt{\varepsilon_{eff}}} \times \sqrt{\left(\frac{m\pi}{a}\right)^2 + \left(\frac{n\pi}{b}\right)^2} \qquad (1)$$

In (1), c is 3×10^8 m/s, and ε_{eff} is the effective permittivity of the FR4 substrate. Note that (1) is an approximate formula to predict the operating frequencies of two CP modes for this designed slot antenna, and they would have obvious errors when the width (W_1) of the ring ground plane is too narrow [19]. A CPW F-shaped feeding structure was set to excite the antenna to achieve low-profile. As shown in Figure 1(a), L_2 mainly contributes to TE_{10} mode while L_3 mainly contributes to TE_{01} mode, with equal amplitudes and 90-degree phase difference caused due to the disturb of L_s, and the circular polarization thus be obtained. L_4 acts as a tuning stub to adjust the input impedance so as to obtain broadband impedance bandwidth which will be discussed in next section.

3. EXPERIMENT VERIFICATION AND DISCUSSION

Figure 3 shows the simulated and measured S_{11} and axial ratio (in the bore-sight direction) of the antenna in Figure 2(a) and Figure 2(b).

The measurements were carried out using Agilent 8753E network analyzer. A good agreement was obtained between the simulated and experimental results. As shown in Figure 3(a), the center

(a) Antenna 1 (proposed)   (b) Antenna 2
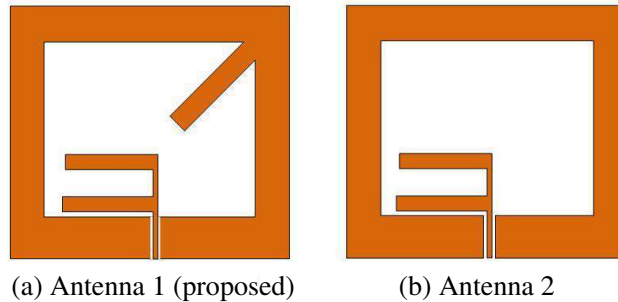
Figure 2. (a) Geometry of the proposed antenna. (b) Geometry of the antenna without spur line along diagonal.

(a)   (b)
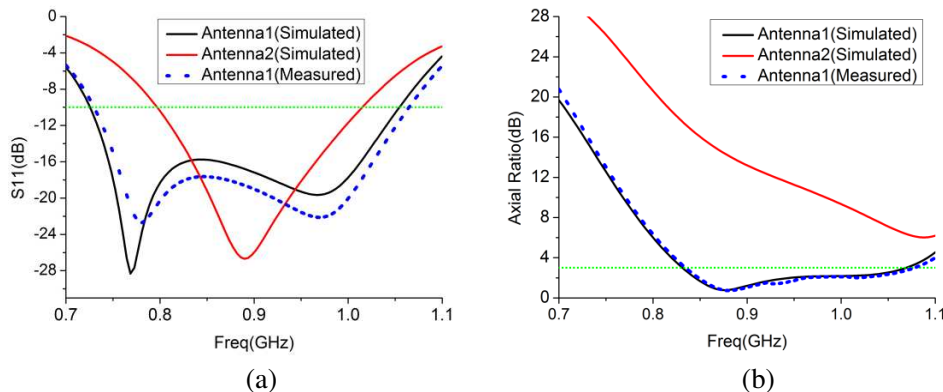
Figure 3. S_{11} and axial ratio for the antenna 1 (proposed) and antenna 2. (a) S_{11}. (b) AR.

frequency of antenna 2 is designed at $f_0 = 890\,\text{MHz}$ as prior calculation. The measured S_{11} of antenna 1 (proposed) is less than $-10\,\text{dB}$ over the frequency range of $733 \sim 1040\,\text{MHz}$ (34.6%). Figure 3(b) exhibits the simulated and measured axial ratios in the bore-sight direction. The measured 3 dB AR bandwidth of 838–1070 MHz or 24.3% is obtained.

The simulated and measured RHCP/LHCP radiation patterns by using an anechoic chamber in XZ- and YZ-planes at different frequencies are plotted in Figure 4, and good symmetry of bidirectional
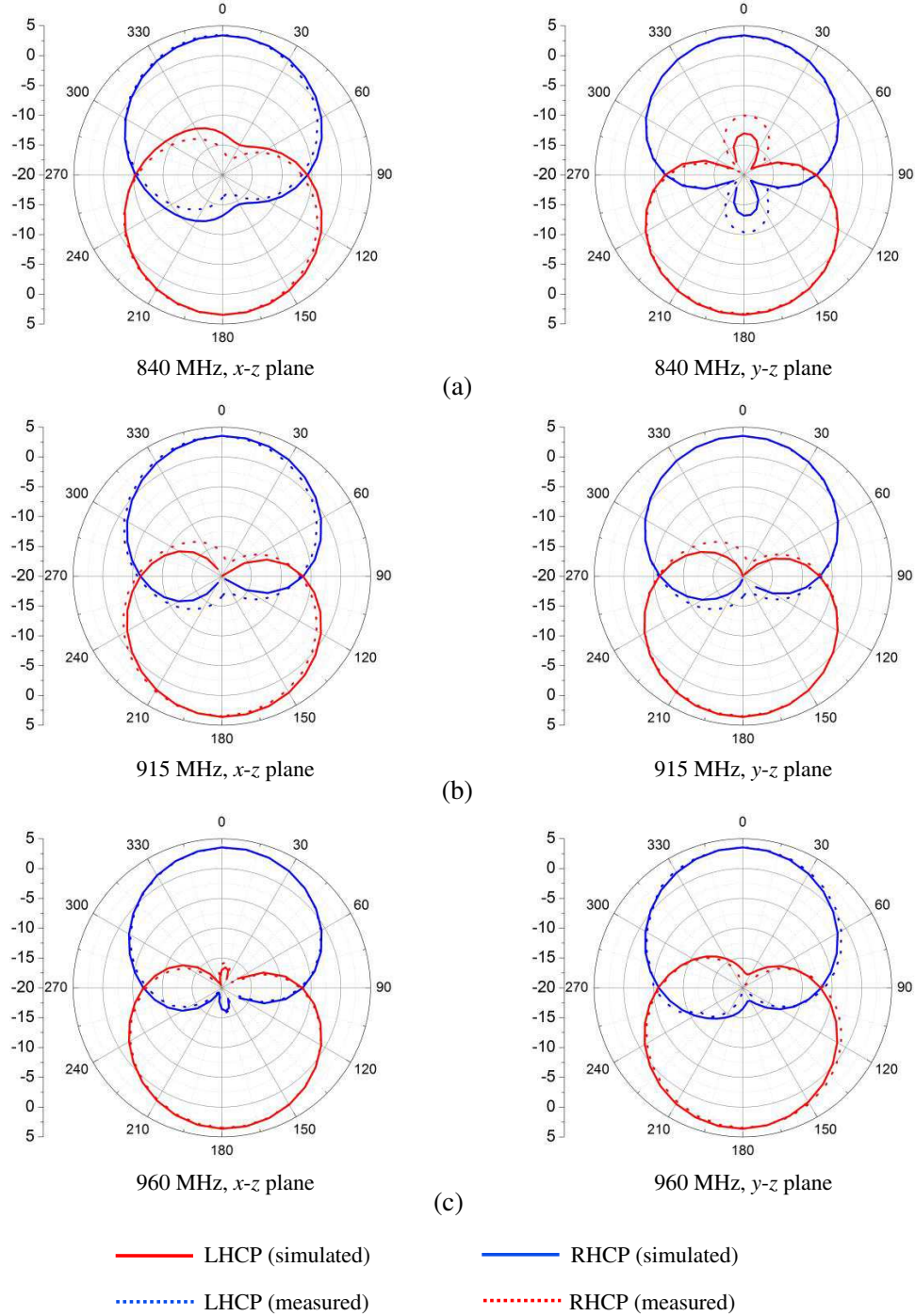
Figure 4. The simulated and measured LHCP/RHCP radiation patterns of proposed antenna in x-z and y-z planes. (a) 840 MHz. (b) 915 MHz. (c) 960 MHz.

radiation has been observed. The measured radiation patterns in the two sides of the proposed antenna are symmetry with contrary circular polarization which is consistent with the prior analysis. Also, it can be observed from the pattern that the minimum 3 dB axial ratio beamwidth over the frequency range of 840 MHz $\sim$ 960 MHz is about 105° ($-45° \sim 60°$) in XZ-plane and 96° ($-44° \sim 52°$) in YZ-plane, which are wider than that in [19], meaning that the tag of the RFID system can be recognized in a wider angle range in both $+\hat{z}$ direction and $-\hat{z}$ direction, that is to say, the number of needed reader in some applications can be reduced.

Parametric studies are also conducted to provide more detailed information about the antenna design. To better understand the influence of the parameters on the performance of the antenna, only one parameter at a time will be varied, while others remain unchanged unless especially indicated.

3.1. Effects of the Spur Line

In this study, by properly adjusting the length and the width of the spur line to lengthen the excited $\hat{x}$-directed patch surface current path, two near-degenerated resonant modes with 90-degree phase difference are excited to form a wide CP operating bandwidth over the UHF band. Figure 5(b) and Figure 5(d) show clearly that two lowest axial ratio values at adjacent frequency points being integrated together so that the AR bandwidth is enhanced as discussed in Section 2.

Figure 5 also shows that the operating frequency increases with the increasing L_s. Moreover, the performance of S_{11} and AR are improved at higher frequency and deteriorated at lower frequency because of the phase delay of $\hat{x}$-directed patch surface enhanced with the increase of L_s. The impact of W_s on AR is similar to that of L_s. The bandwidth less than 3 dB AR can totally satisfy the specification of UHF band when the values of L_s and W_s are set to 58.5 mm and 10 mm, respectively.
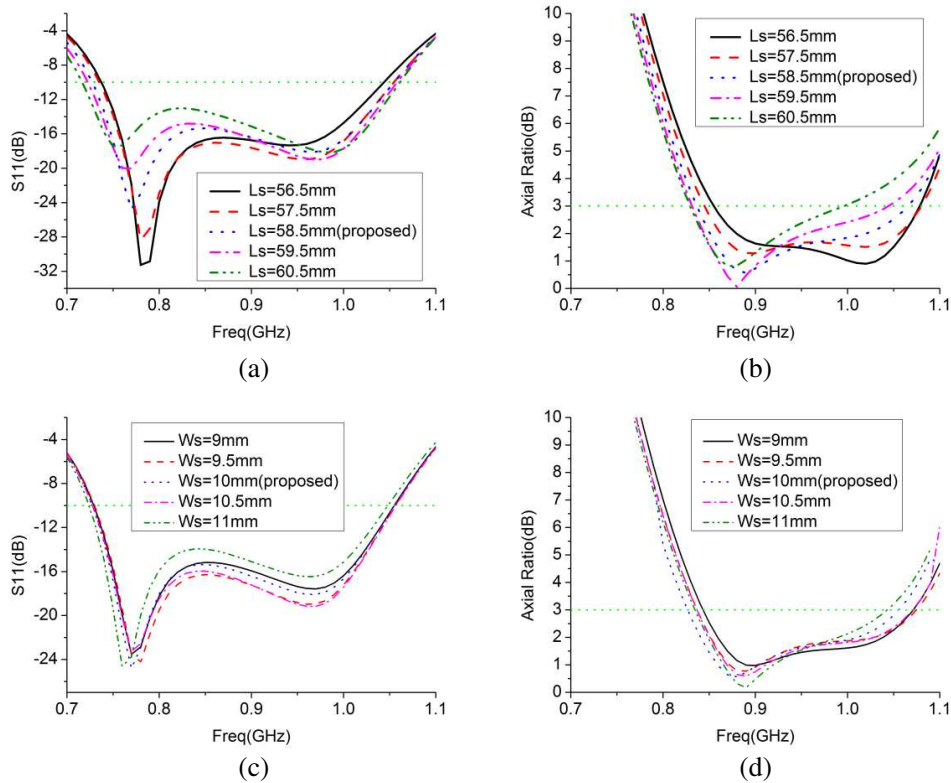
Figure 5. Simulated results against frequency of the proposed antenna with various L_s and W_s. (a) Simulated results of S_{11} varies with the length of L_s. (b) Simulated results of AR varies with the length of L_s. (c) Simulated results of S_{11} varies with the width of W_s. (d) Simulated results of AR varies with the width of W_s.

3.2. Effects of the F-shaped Feeding Structure

Figure 6 shows that the resonant point of the proposed antenna moves with the various gap (G). It is obvious that the resonant point moves up with the increasing gap resulting from the decrease of the capacitive couple between the F-shaped feeding structure and square slot. The value of the gap is set at 0.5 mm to cover the whole band of UHF RFID from 840 MHz to 960 MHz. The value of the gap makes slight impact on axial ratio as shown in Figure 6(b).

The lengths of L_2, L_3 and L_4 make slight influence on AR as shown in Figure 7(b), Figure 7(d) and Figure 7(f). Figure 7(a) and Figure 7(c) show that the value of S_{11} varies with different lengths of L_2 and L_3 due to the resonant points shifting with the whole length of $L_2 + L_3$. Also, Figure 7(e) shows

(a)   (b)
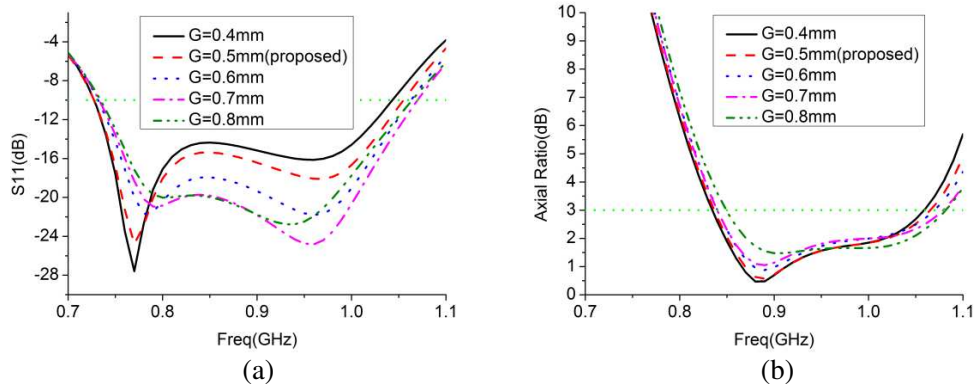
Figure 6. Simulated results against frequency for the proposed antenna with various value of gap (G). (a) S_{11}. (b) Axial ratio.

(a)   (b)

(c)   (d)
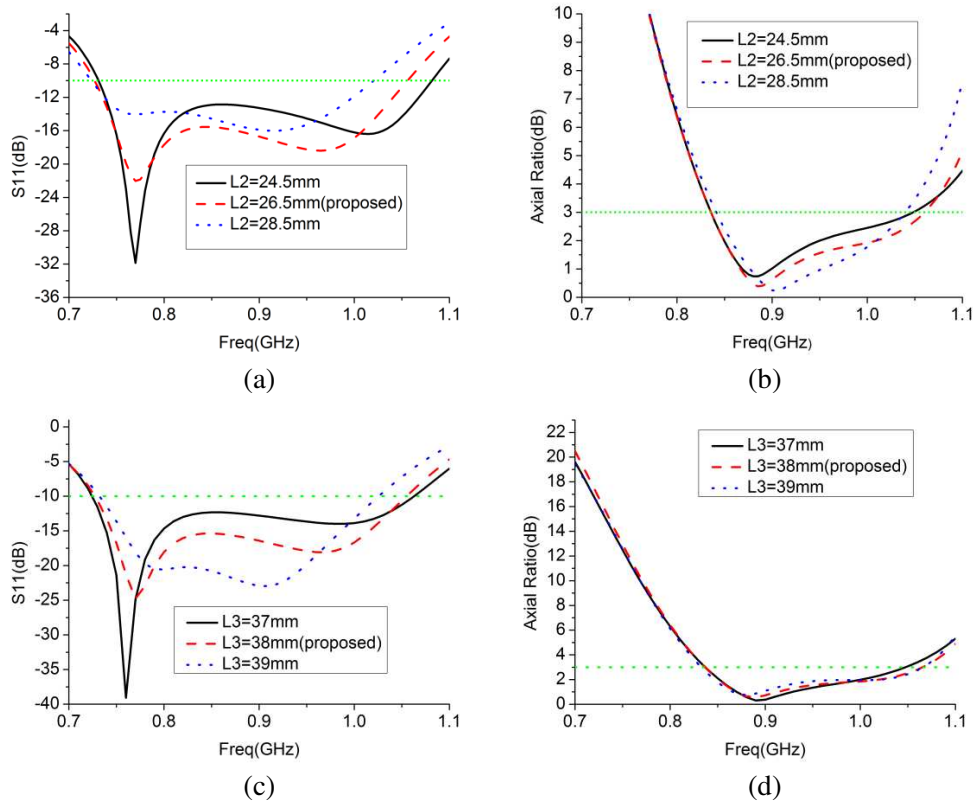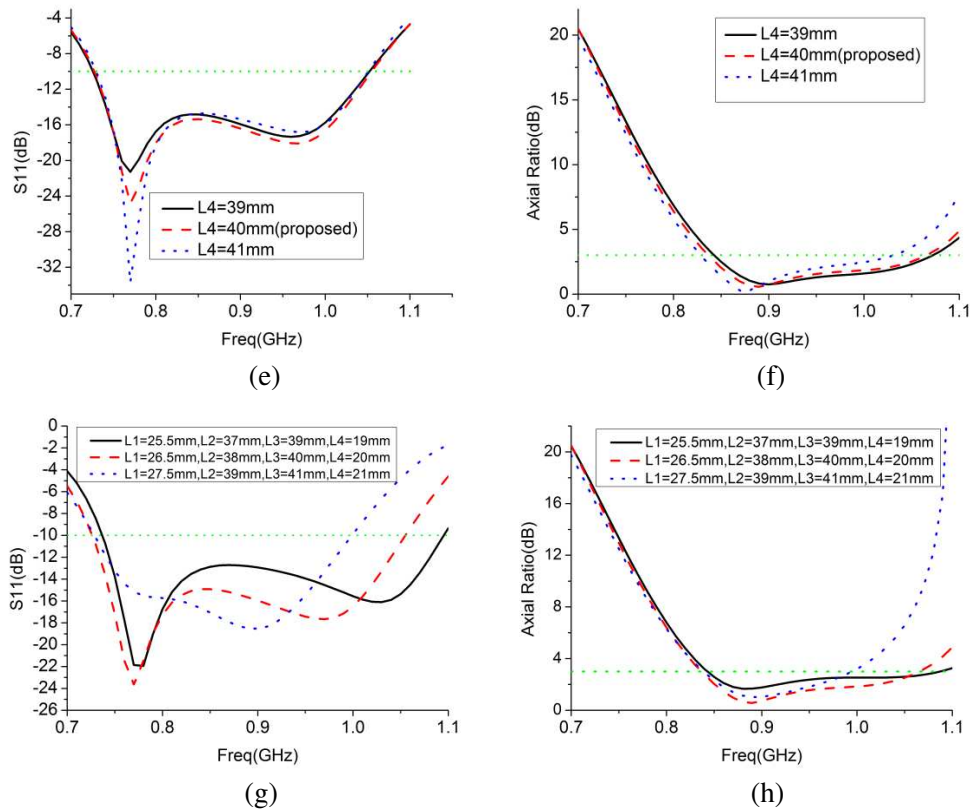
Figure 7. Simulated results of S_{11} and AR against frequency with various of L_2 and L_4. (a) Simulated results of S_{11} varies with the length of L_2. (b) Simulated results of AR varies with the length of L_2. (c) Simulated results of S_{11} varies with the length of L_3. (d) Simulated results of AR varies with the length of L_3. (e) Simulated results of S_{11} varies with the length of L_4. (f) Simulated results of AR varies with the length of L_4. (g) Simulated results of S_{11} with simultaneous variation of L_1, L_2, L_3 and L_4. (h) Simulated results of AR with simultaneous variation of L_1, L_2, L_3 and L_4.

that L_4 acts as the tuning stub to adjust the input impedance. The length of L_4 makes impact on the minimum value of S_{11} because the coupling between L_4 and square slot decreases with the decreasing length of L_4. With the different lengths of L_4, S_{11} is modified to satisfy the specification across the whole UHF band. The impacts of simultaneous variation of L_1, L_2, L_3 and L_4 on S_{11} and AR are also analyzed to verify the influence of the feeding structure. As shown in Figure 7(g) and Figure 7(h), S_{11} and AR degenerate simultaneously at higher frequency band because the operating frequency is shifted down with the increase of the total length of $L_1 + L_2 + L_3$.

4. CONCLUSION

A compact broadband CPW-fed CP antenna has been presented for UHF RFID applications in this paper. By using an F-shaped structure and square slot embedded with a spur line along diagonal, the optimized antenna has achieved the desired performance over the UHF band of 840–960 MHz with the gain of more than 3.6 dBic, AR of less than 3 dB, return loss of less than 15 dB, and 3 dB AR beamwidth of larger than 90 degrees with nearly bidirectional pattern in the XZ- and YZ-plane. The great performance makes it a good candidate for the UHF RFID applications worldwide, and the information derived from the study will be helpful for antenna engineers to design and optimize the antennas for UHF RFID applications. The proposed antenna will be beneficial for RFID system configuration and implementation, as well as cost reduction.

REFERENCES

1. Kim, M. and K. Kim, "Automated RFID-based identification system for steel coils," *Progress In Electromagnetics Research*, Vol. 131, 1–17, 2012.

2. Want, R., "An introduction to RFID technology," *IEEE Pervasive Comput.*, Vol. 5, No. 1, 25–33, Jan.–Mar. 2006.

3. Finkenzeller, K., *RFID Handbook*, 2nd Edition, Wiley, New York, 2004.

4. Tiang, J.-J., M. T. Islam, N. Misran, and J. S. Mandeep, "Circular microstrip slot antenna for dual-frequency RFID application," *Progress In Electromagnetics Research*, Vol. 120, 499–512, 2011.

5. Chen, S.-L., S.-K. Kuo, and C.-T. Lin, "A metallic RFID tagdesign for steel-bar and wire-rod management application in thesteel industry," *Progress In Electromagnetics Research*, Vol. 91, 195–212, 2009.

6. Lai, X.-Z., Z.-M. Xie, and X.-L. Cen, "Design of dual circularly polarized antenna with high isolation for RFID application," *Progress In Electromagnetics Research*, Vol. 139, 25–39, 2013.

7. Amin, Y., Q. Chen, L.-R. Zheng, and H. Tenhunen, "Development and analysis of flexible UHF RFID antennas for 'green' electronics," *Progress In Electromagnetics Research*, Vol. 130, 1–15, 2012.

8. Chang, T. N. and J. M. Lin, "A novel circularly polarized patch antenna with a serial multislot type of loading," *IEEE Trans. Antennas Propag.*, Vol. 55, 3345–3348, 2007.

9. Deng, J.-Y., L.-X. Guo, T.-Q. Fan, Z.-S. Wu, Y.-J. Hu, and J.-H. Yang, "Wideband circularly polarized suspended patch antenna with indented edge and gap-coupled feed," *Progress In Electromagnetics Research*, Vol. 135, 151–159, 2013.

10. Wang, P., G. Wen, J. Li, Y. Huang, L. Yang, and Q. Zhang, "Wideband circularly polarized UHF RFID reader antenna with high gain and wide axial ratio beamwidths," *Progress In Electromagnetics Research*, Vol. 129, 365–358, 2012.

11. Tiang, J.-J., M. T. Islam, N. Misran, and J. S. Mandeep, "Circular microstrip slot antenna for dual-frequency RFID application," *Progress In Electromagnetics Research*, Vol. 120, 499–512, 2011.

12. Ooi, P. C. and K. T. Selvan, "A dual-band circular slot antenna with an offset microstrip-fed line for PCS, UMTS, IMT-2000, ISM, bluetooth, RFID and WLAN applications," *Progress In Electromagnetics Research Letters*, Vol. 16, 1–10, 2010.

13. Chen, Z., X. Qing, and L. Hang, "A universal UHF RFID reader antenna," *IEEE Trans. Microw. Theory Tech.*, Vol. 57, 1275–1282, 2009.

14. Nasimuddin, Z. Chen, and X. Qing, "Asymmetric-circular shape slotted microstrip antennas for circular polarization and rfid applications," *IEEE Trans. Antennas Propag*, Vol. 58, 3821–3828, 2010.

15. Chen, J.-P. and P. Hsu, "A spirally complementary split-ring resonators antenna for circular polarization and RFID reader application," *2012 IEEE Antennas and Propagation Society International Symposium (APSURSI)*, 1–2, 2012.

16. Wang, Z., S. Fang, S. Fu, and S. Jia, "Single-fed broadband circularly polarized stacked patch antenna with horizontally meandered strip for universal UHF RFID applications," *IEEE Trans. Microw. Theory Tech.*, Vol. 59, 1066–1073, 2011.

17. Chen, H.-D., "Broadband CPW-fed square slot antennas with a widened tuning stub," *IEEE Trans. Antennas Propag.*, Vol. 51, 1982–1986, 2003.

18. Yeh, S.-A., Y.-F. Lin, H.-M. Chen, and J.-S. Chen, "Slotline-fed circularly polarized annular-ring slot antenna for RFID reader," *Asia Pacific Microwave Conference, APMC 2009*, 618–621, 2009.

19. Lu, J.-H. and S.-F. Wang, "Planar broadband circularly polarized antenna with square slot for UHF RFID reader," *IEEE Trans. Antennas Propag.*, Vol. 61, 45–53, 2013.